

physica **p** status **s** solidi **S**

www.interscience.wiley.com

reprints

The collage features five journal covers:

- physica status solidi **a**** (www.pss-a.com): Applications and materials science. Editor's Choice: Highly efficient all-nitride phosphor-converted white light emitting diode (Regina Mueller-Mach et al., p. 1727). Includes a diagram of a light-emitting diode structure.
- physica status solidi **b**** (www.pss-b.com): Basic solid state physics. Current Trends in Electronic Structure: Embedding and Linear Scaling Techniques (Thomas Beck, and Eduardo Hernandez). Includes a diagram of a crystal lattice.
- physica status solidi **c**** (www.pss-c.com): Current topics in solid state physics. Includes a photograph of a glowing material.
- physica status solidi **rrl**** (www.pss-rapid.com): Rapid research letters. Includes a diagram of a crystal structure.
- physica status solidi **a**** (www.pss-a.com): Applications and materials science. Includes a diagram of a light-emitting diode structure.

Additional text on the collage includes:

- www.pss-b.com
- www.pss-c.com
- www.pss-rapid.com
- WILEY-VCH logo
- InterScience logo
- SPECIAL ISSUE

Hidden structure in amorphous solids

F. Inam¹, James P. Lewis², and D. A. Drabold^{*1,3}

¹Department of Physics and Astronomy, Ohio University, Athens, Ohio 45701, USA

²Department of Physics, West Virginia University, Morgantown, West Virginia 26506, USA

³Trinity College, Cambridge CB2 1TQ, UK

Received 6 August 2009, revised 6 November 2009, accepted 8 November 2009

Published online 5 February 2010

PACS 31.15.ae, 61.43.Bn, 61.43.Dq, 71.23.Cq

* Corresponding author: e-mail drabold@ohio.edu, Phone: (+1) 740 593 1715, Fax: (+1) 740 593 0433

Recent theoretical studies of amorphous silicon (a-Si) [Pan et al., Phys. Rev. Lett. **100**, 206403 (2008)] have revealed subtle but significant structural correlations in network topology: the tendency for short (long) bonds to be spatially correlated with other short (long) bonds). These structures were linked to the

electronic band tails in the optical gap. In this paper, we further examine these issues for a-Si, and demonstrate that analogous correlations exist in amorphous SiO₂, and in the organic molecule, β -carotene. We conclude with a discussion of the origin of the effects and its possible generality.

© 2010 WILEY-VCH Verlag GmbH & Co. KGaA, Weinheim

1 Introduction The continuous random network (CRN) has become the accepted model for homogeneously disordered materials, and for good reason: such atomistic models reproduce the experimentally observed properties of the materials, including some of the finer details, such as the Urbach tailing in the electronic density of states [1–4].

Recently [5], we have closely examined some particularly realistic CRN models of amorphous silicon (a-Si), and reported that there are subtle correlations that have not been previously noted: short bonds tend to be connected to other short bonds and an analogous statement for long bonds. In a-Si, the longer bonds form filamentary (1D) structures, and the short bonds tend to cluster in a higher dimensional way, albeit with some 1D character. We have shown that the Urbach tails in the electronic density of states arise from these structures [4] (the valence tail associated with the short bonds, conduction tail with long bonds).

The purpose of this paper is to explore the case of a-Si a bit farther, and to look for related phenomena in glasses (silica) and beyond. Obvious questions include: (1) Are “filaments” universal? (2) Do these topologic features offer a general explanation for the origin of the Urbach tails? (3) Why do these structures form, and can they be manipulated to tailor the band tails in a useful way? We do not offer complete answers to these questions, but provide new information relevant to all three.

2 Methods Where a-Si is concerned, we focus our attention on a 512-atom model due to Djordjevic, Thorpe,

and Wooten (DTW) [6], made using the Wooten–Weaire–Winer (WWW) approach [1]. The DTW model is thoroughly relaxed within the WWW scheme, and to our knowledge, is not in significant contradiction with any experiment (structural, electronic, or vibrational). The model has perfect fourfold coordination. We have relaxed the model with an accurate *ab initio* code and find tiny rearrangements, with no bond breaking or formation. Where subtle or “hidden” structural correlations are concerned, we have discussed this (and eight other models made in various ways) in detail elsewhere [5].

We look for analogous structural and electronic correlations in a-SiO₂. For a-SiO₂, we start with a 648-atom Decorate and Relax model in excellent agreement with experiment [7].

All electronic structure and force calculations are implemented with SIESTA, a standard first principles, local basis code. We updated the model of amorphous silica by relaxing it with a highly optimized double-zeta-polarized basis in SIESTA, kindly provided by E. Artacho. Changes were small compared to the published model.

3 a-Si: Short recapitulation Previous work [4, 5] on a-Si demonstrated that: (1) long and short bonds are spatially correlated, short favoring proximity with short, and long with long. Furthermore, the long bond structures are filamentary, whereas the short bonds tend to cluster in 3D (see Fig. 1). There is little or no cross-correlation (long bond to short bond); (2) the electronic valence tails arise from short

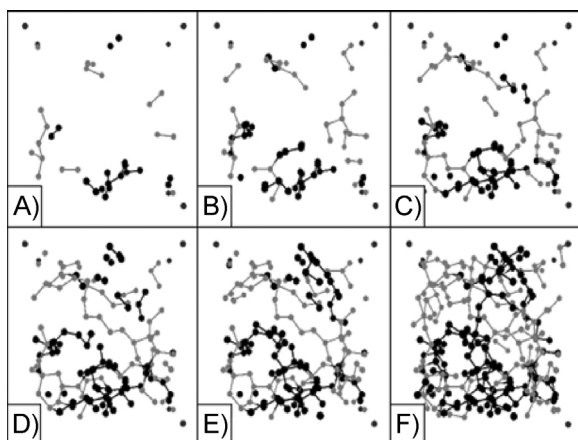


Figure 1 (A) 1%, (B) 2%, (C) 3% (D) 4% (E) 5%, and (F) 8% longest (light) and shortest (dark) bonds in 512-atom DTW model [6] of a-Si (from Ref. [5]).

bonds and the conduction tails from long bonds; (3) energies close to the Fermi level (E_f) are localized on the longest (for energies slightly above E_f) and shortest bonds (for energies slightly below E_f); (4) if the network is changed to eliminate the short-short and long-long correlations (but no bonds are broken or formed) the model does *not* yield an exponential density of states; and (5) simulations of relaxed point defects (Si divacancy) in diamond show a filamentary structure upon relaxation, and hint at the formation of an exponential tail, in apparent agreement with ion-bombardment experiments, that reveal an Urbach edge before amorphization [4].

4 a-Si: Defect nuclei To quantitatively characterize the long or short bonds and their associated strain or relaxation field, we look at how bond lengths vary as a function of distance from the defect center or “nucleus” – by this we refer to a central bond smaller (or larger) than any nearby. In Fig. 2, we show the characteristic length of a particular short-bond cluster. Λ is the longest distance to

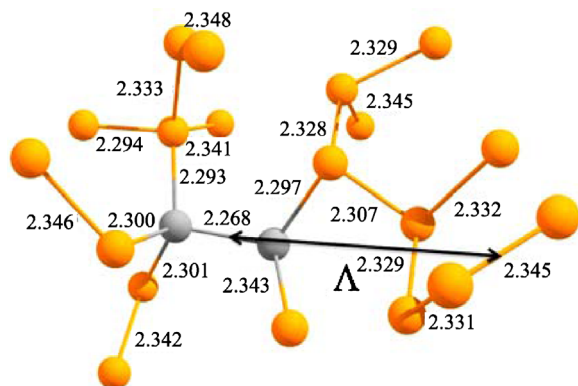


Figure 2 (online color at: www.pss-a.com) Example of a short-bond cluster in a-Si. Λ : linear extent of densified region induced by defect nucleus (gray bond).

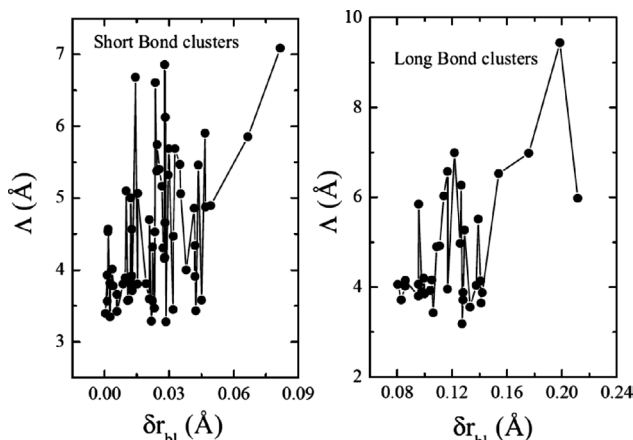


Figure 3 Plot of linear extent of relaxed defect Λ as a function of δr_{bl} , the difference in bond length of the defect nucleus from the mean (2.35 \AA).

sites with a normal bond length. We repeat this analysis for many defect nuclei.

In Fig. 3, we plot $\Lambda(\delta r)$, where δr is the deviation from the mean bond length in a-Si (about 2.35 \AA). The plots are noisy (and not to be taken seriously in any case for $\delta r/f \ll 1$, where $f \sim 0.09 \text{ \AA}$ is the FWHM of the a-Si bond length distribution function), but show that for short bonds, Λ becomes large; whereas for bonds longer than the mean, there is no obvious functional dependence: long bonds do not imply a long-range relaxation field.

We further differentiate between the long- and short-bond clusters by computing the number of atoms N_{cl} participating in the deformation caused by a particular nucleus (Fig. 4). Here, the difference between long and short bond cases is stark, reflecting the strong correlation between the relaxation around the short bond defects and the bond

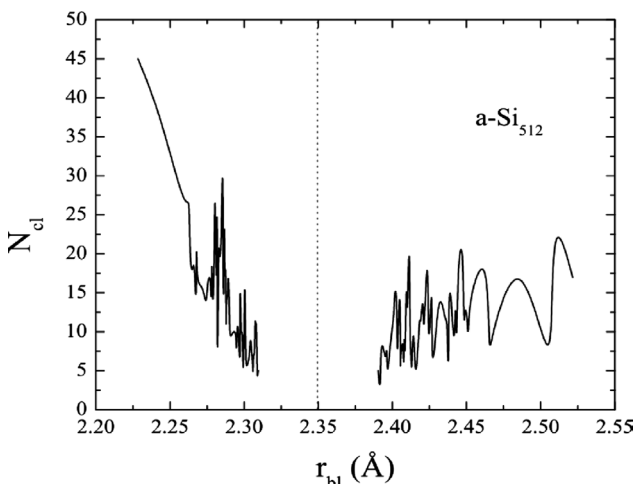


Figure 4 Number of atoms in short-bond and long-bond clusters (N_{cl}) are plotted against the central bond length of the cluster for a-Si. Mean bond length is represented by the dotted.

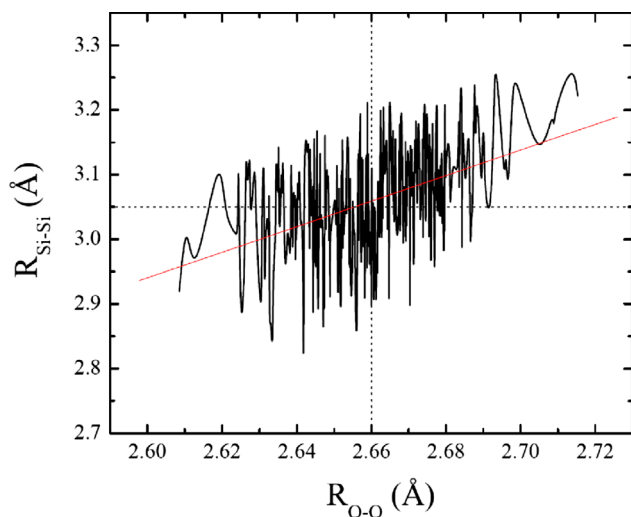


Figure 5 (online color at: www.pss-a.com) Correlation between the two lengths $R_{\text{Si-Si}}$ and $R_{\text{O-O}}$. Diagonal line is a linear fit to the data. Dotted lines indicate the mean values of the two lengths.

length deviation at the nucleus. This implies that in a-Si, the short bond is a seed for growing a local volume of higher density, and the shorter the bond the larger the effect. Roughly speaking, this suggests that if one is able to create a short bond in any fashion, one can expect the network to locally densify around that nucleus.

5 The case of a-SiO₂ The 648-atom a-SiO₂ model is chemically ordered, all Si are fourfold, and all O are twofold. The neutron structure-factor obtained from the model is in excellent agreement with experiments (as are bond angle distributions and other observables) [7]. In this section, we explore the network connectivity of amorphous silica using the methods of the previous sections applied to a-Si. In contrast to a-Si, no topologic correlations were found for the Si–O nearest-neighbor bond lengths. We then considered second-neighbor distances $R_{\text{O-O}}$ (with mean length 2.66 Å) and $R_{\text{Si-Si}}$ (with mean length 3.05 Å). Since the variation in Si–O bond length is tiny (FWHM ~ 0.01 Å), the fluctuation in $R_{\text{O-O}}$ and $R_{\text{Si-Si}}$ is really due to broadening associated with O–Si–O and Si–O–Si angles. The fluctuation in $R_{\text{Si-Si}}$ (FWHM ~ 0.2 Å) is larger than that of $R_{\text{O-O}}$ (FWHM ~ 0.1 Å). Figure 5 indicates a linear dependence between the two lengths. The O sites with shorter $R_{\text{O-O}}$ have shorter $R_{\text{Si-Si}}$, so that smaller $R_{\text{O-O}}$ implies higher densities.

In analogy with our work on a-Si (Fig. 1), we show examples of the connectivity of the subnetwork formed by long and short second neighbors in Fig. 6. Figure 7 shows the correlation between N_{cl} and the short (longer) length clusters of the two kinds. A crudely linear correlation is evident for short $R_{\text{O-O}}$, a trend analogous to the a-Si network. Cluster size N_{cl} also exhibits linear behavior for large $R_{\text{Si-Si}}$. The connectivity of short $R_{\text{O-O}}$ clusters tends to be of a compact 3D nature, while large $R_{\text{Si-Si}}$ clusters are more extended and

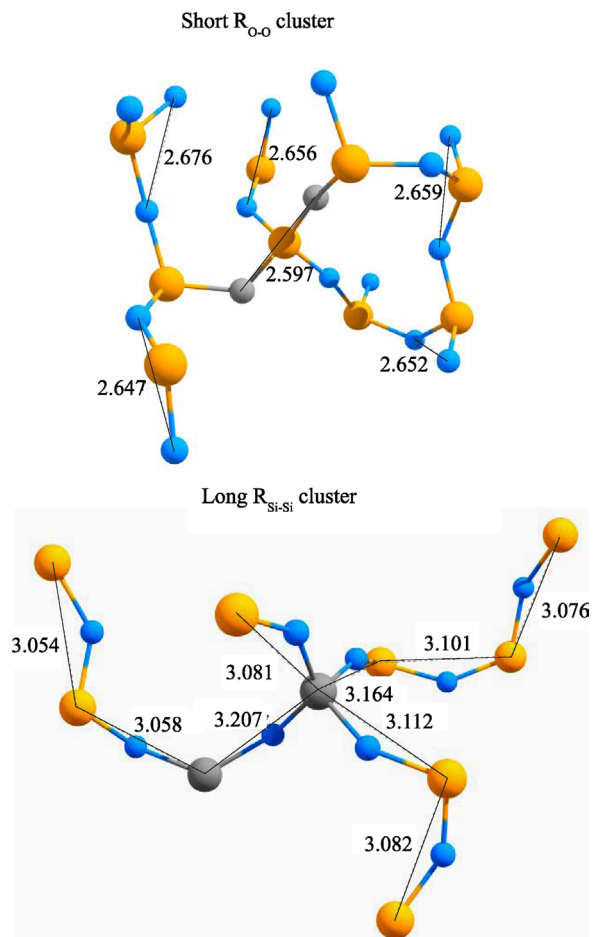


Figure 6 (online color at: www.pss-a.com) Examples of short $R_{\text{O-O}}$ and long $R_{\text{Si-Si}}$ clusters in a-SiO₂ network. Gray sites represent the defect nuclei.

filamentary (1D). The average spatial extension of the small $R_{\text{O-O}}$ clusters is of order 5.0 Å reflecting the denser nature of the surrounding network induced by the defect seed or nucleus.

The link between topology of the network and the electronic spectrum is analyzed by calculating the symmetrized charge-weighted lengths defined by:

$$R(E) = \frac{\sum_{l,m,n} \rho(l,n) q(l,E) q(m,E) q(n,E)}{\sum_{l,m,n} q(l,E) q(m,E) q(n,E)}, \quad (1)$$

where $\rho(l,n)$ is the distance between two second-neighbor sites l and n with shared site m between them and q is the charge computed from the electronic wave function (Kohn–Sham orbital) on a particular site for eigenenergy E . The mean deviation $\delta(E) = R(E) - R_0$, and R_0 is the average length for (either $R_{\text{O-O}}$ or $R_{\text{Si-Si}}$). In addition, the inverse participation ratio (IPR), a gauge of electronic localization, is shown in Fig. 8. An asymmetric contribution from the short $R_{\text{O-O}}$ and long $R_{\text{Si-Si}}$ lengths at the band tails is

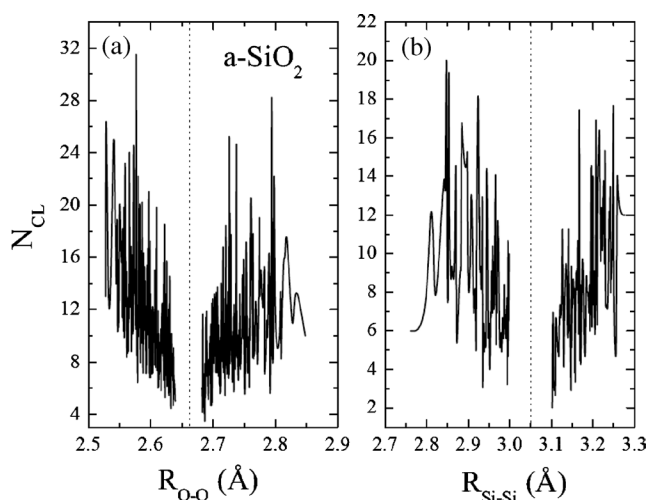


Figure 7 N_{cl} as a function of second-neighbor distances (see text). Vertical lines are mean-distances.

apparent. The localized valence tail states are clearly correlated to the short R_{O-O} lengths and localized conduction tails associated with long Si–Si second neighbor distances.

The correlation between the denser volumes, characterized by the short R_{O-O} lengths, and the valence tail states in a-SiO₂ system is reminiscent to the case of a-Si, and perhaps suggests a simple and broadly applicable understanding of the network origins of the Urbach edge, and the nature of the defect-induced strain field in disordered systems.

6 Farther afield There are indications that some of the effects we report here occur in (apparently) very different

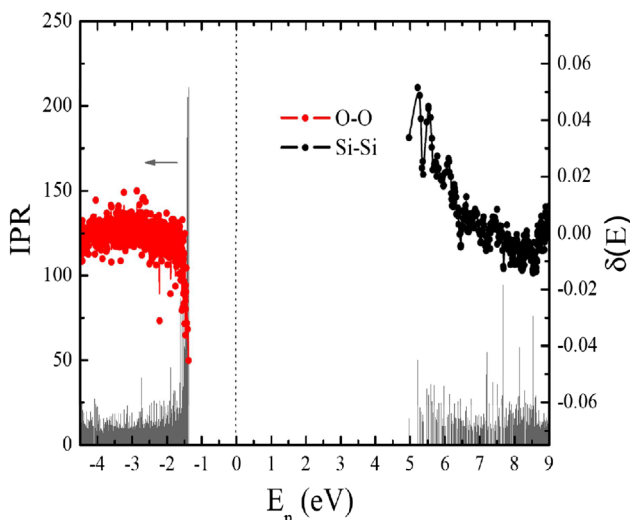


Figure 8 (online color at: www.pss-a.com) Bond length decomposition of density of states for amorphous silica. Dotted line indicates Fermi level. The valence (conduction) edge is dominated by short O–O bonds (long Si–Si bonds).

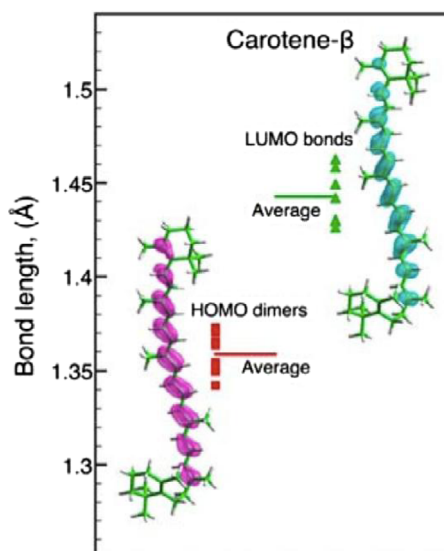


Figure 9 (online color at: www.pss-a.com) HOMO (purple) and LUMO (cyan) states correspond to short and long bonds, with mean bond length 1.36 Å (1.44 Å) for HOMO (LUMO).

systems. Thus, in the important conjugated organic compound β -carotene ($C_{40}H_{56}$) a similar tendency is observed. In Fig. 9, we reproduce these results. The highest occupied molecular orbital (HOMO) state and lowest unoccupied molecular orbital (LUMO) state may be viewed as molecular analogs to the valence and conduction tails, respectively. The charge-weighted bond length $R(E)$ for the HOMO (LUMO) is 1.36 Å (1.44 Å), respectively.

Both experiment and computation show that the conjugation length (i.e., the number of coplanar rings in a π -system, which in turn determines the overlap strength of the π orbitals) in β -carotene is 9.7, despite the fact that there are eleven double bonds in the molecule. The HOMO orbital is tied to the shortened double bonds. Preliminary results on β -carotene suggest that frontier orbitals are localized at conjugation sites and may also contribute to lowering of the HOMO energy, compensating increase in energy due to the shortening of the double bonds (Fig. 9).

7 Discussion The systems we have discussed in this paper have only a few things in common. One is that all include disorder. A second feature is that all are relaxed to a minimum of suitable energy functionals (in this paper, always *ab initio*).

The consequence of a local densification around a short bond is quite plausible: the relaxation of the network around the nucleus is the strain field associated with the defect. Of course there is no similar statement for a long bond – a very long bond is a broken bond; the system does not become diffuse with long bonds, it reconstructs and forms voids.

In a-Si, the decay length for the spatial correlations from a nucleus is ~ 7 Å. It is interesting that this distance is quite similar to the range of the density matrix in the material (for a

review, see Ref. [8]). The latter is a measure of the spatial locality of quantum mechanics in a particular material, and also the range required of an accurate interatomic potential (specifically, the electronic contribution to the potential energy). Consistent with this observation, we note that the characteristic defect nucleus relaxation scale of a-SiO₂ is smaller, something like 5 Å, consistent with the larger optical gap in silica, which is the prime determinant of the range of interatomic interactions.

The observation that short bond lengths are associated with valence tail states and long with conduction states is not a surprise. Within the usual tight-binding picture, the valence states are of bonding character and the conduction states of anti-bonding character, which leads naturally to the qualitative association of shorter bonds with valence states and longer with conduction. The following points substantially clarify this intuitive view: (1) in a purely covalent material (a-Si) the function $R(E)$ (Eq. 1) is remarkably symmetric about E_f [4, 5]; (2) the closer to E_f , the shorter (longer) the associated bonds on the valence (conduction) side of the Fermi level; and (3) the short or long bonds are spatially correlated.

In connection with point (3), one might suppose *a priori* that the short or long bonds are randomly distributed in space. If this was so, the wave functions just above or below E_f would be rather strange, with weight randomly dispersed over the network. But minimizing the energy in quantum mechanics is famously a “balancing act”: the electronic energy is the sum of kinetic and potential energy terms. Thus, we conclude from these calculations that the kinetic energy term, which always favors delocalization, succeeds in “connecting up” the long or short bonds, albeit in a $\sim 1D$ fashion for the former and a higher dimension for the latter. This suggests a “chicken and egg” problem: does the network organize itself (with structural blobs and filaments) to enable the electrons to reduce the Laplacian term (and delocalize electrons), or is the existence of structural blobs and filaments a consequence of minimizing the total energy (ions + electrons)? As we indicated above, it seems that some simple empirical potentials (even Keating springs) lead to structural blobs and filaments. To the extent that the empirical potentials themselves are constructed to reproduce experimental facts about the system (which in turn depend upon the electronic contribution to the total energy), perhaps the answer is not altogether clear.

A key feature of electron localization is that it creates a link between an electronic energy and a structural entity in a model. Thus, we observe valence tail states (i.e., energy eigenstates from a specific narrow energy range) localized on blob-like regions. An analogous statement applies to filaments for conduction tail states. This has the interesting consequence that it causes Figs. 7 and 8 to be related. In fact the quantity N_{cl} is very much like a participation ratio. This paper shows that there is a close connection between R_{O-O} , R_{Si-Si} and the electronic energy E of Fig. 8. Thus, we show, for example, that dense regions in amorphous silica will particularly affect the valence tail, and lower

density volumes will preferentially impact the conduction tail.

From an electronic point of view the existence of blobs and filaments associated with the quantum localized-to-extended transition has been demonstrated in realistic calculations for a-Si [9]. These papers sought to characterize the localized to extended transition in a real material (with the disorder being computed from realistic structural models). They clearly showed the blob + filament nature of states near the Fermi level. The weakness of these calculations is that the models are relatively small (so far up to 10^4 atoms), whereas the 3D Anderson model has been diagonalized for systems exceeding 10^7 atoms [10]. For such large systems, it becomes possible to compute the fractal dimension for the critical eigenstates (the result is not far from $D = 1.3$, though there continuing dispute about the exact value). Qualitatively, our work shows that on the conduction side of the Fermi level states are quite filamentary ($D = 1+$) and on the valence side something distinctly higher, say $D = 3-$. The value of the fractal dimension at criticality is unknown for a real system in 3D.

Finally, we note that Phillips’ model [11] for cuprate superconductivity emphasizes the importance of the filamentary states of the type we have detected in a-Si and a-SiO₂. Interestingly, atomic-resolution tunneling asymmetry experiments on the cuprates have observed states with topology qualitatively like what we report here [12, 13]. Given the appearance of blobs and filaments (both topologic and electronic) in the diverse range of systems described here, and the known importance of disorder on the properties of the cuprates, we think this work lends some support to Phillips’ view.

Acknowledgements We thank the US Army Research Office and US Army Research Lab for supporting this work, accomplished under cooperative agreement W911NF-0-2-0026 within the MURI program and the US NSF under grant DMR 0903225. We thank S. Chakraborty for supporting calculations on a-SiO₂, and Dr. J. C. Phillips for helpful comments and encouragement. DAD thanks the US NSF and the Leverhulme Trust (UK) for sabbatical support. We thank Prof. Emilio Artacho for providing us with a carefully optimized basis set for SiO₂, and Prof. S. R. Elliott for many conversations and hospitality.

References

- [1] F. Wooten, K. Winer, and D. Weaire, Phys. Rev. Lett. **54**, 1392 (1990).
- [2] P. Biswas, D. N. Tafen, F. Inam, B. Cai, and D. A. Drabold, J. Phys.: Condens. Matter **21**, 084207 (2009).
- [3] J. Dong and D. A. Drabold, Phys. Rev. Lett. **80**, 1928 (1998).
- [4] Y. Pan, F. Inam, M. Zhang, and D. A. Drabold, Phys. Rev. Lett. **100**, 206403 (2008).
- [5] Y. Pan, M. Zhang, and D. A. Drabold, J. Non-Cryst. Solids **354**, 3480 (2008); see also P. A. Fedders, D. A. Drabold, S. Nakhmanson, Phys. Rev. B **58**, 15624 (1998).
- [6] B. R. Djordjevic, M. F. Thorpe, and F. Wooten, Phys. Rev. B **52**, 5685 (1995).

- [7] D. Tafen and D. A. Drabold, *Phys. Rev. B* **71**, 054206 (2005).
- [8] D. A. Drabold, *Eur. Phys. J. B* **68**, 1 (2009); X. Zhang and D. A. Drabold, *Phys. Rev. B* **63**, 233109 (2001).
- [9] J. Ludlam, S. N. Taraskin, S. R. Elliott, and D. A. Drabold, *J. Phys.: Condens. Matter* **17**, L321 (2005).
- [10] O. Schenck, O. Bollhofer, and R. A. Romer, *SIAM Rev.* **50**, 91 (2008).
- [11] J. C. Phillips, *Phys. Rev. B* **75**, 214503 (2007), and references therein.
- [12] Y. Kohsaka, C. Taylor, K. Fujita, A. Schmidt, C. Lupien, T. Hanaguri, M. Azuma, M. Takano, H. Eisaki, H. Takagi, S. Uchida, and J. C. Davis, *Science* **315**, 1380 (2007).
- [13] M. C. Boyer, W. D. Wise, K. Chatterjee, M. Yi, T. Kondo, T. Takeuchi, H. Ikuta, and E. W. Hudson, *Nat. Phys.* **3**, 802 (2007).